Journal of Pharmaceutical Analysis 14 (2024) 100903

Contents lists available at ScienceDirect

Journal of Pharmaceutical Analysis

journal homepage: www.elsevier.com/locate/jpa

Original article

An environmentally sensitive zinc-selective two-photon NIR fluorescent turn-on probe and zinc sensing in stroke

Junfeng Wang [a, b, *, 1], Qibing Liu [c, d, 1], Yingbo Li [e, 1], Yi Pang [a, f, **]

[a] Department of Chemistry, The University of Akron, Akron, OH 44325, USA
[b] Gordon Center for Medical Imaging, Department of Radiology, Massachusetts General Hospital, Harvard Medical School, Boston, MA 02114, USA
[c] Department of Pharmacy, The First Affiliated Hospital of Hainan Medical University, Haikou, 570100, China
[d] Engineering Research Center of Tropical Medicine, Ministry of Education, Hainan Medical University, Haikou, 571199, China
[e] State Key Laboratory of Natural and Biomimetic Drugs, School of Pharmaceutical Sciences, Peking University, Beijing, 100191, China
[f] Maurice Morton Institute of Polymer Science, The University of Akron, Akron, OH 44325, USA

ARTICLE INFO

Article history:
Received 5 August 2023
Received in revised form
1 November 2023
Accepted 21 November 2023
Available online 29 November 2023

Keywords:
Near-infrared
Molecular imaging
Thrombus
Stroke

ABSTRACT

A two-photon near infrared (NIR) fluorescence turn-on sensor with high selectivity and sensitivity for Zn^{2+} detection has been developed. This sensor exhibits a large Stokes' shift (~300 nm) and can be excited from 900 to 1000 nm, with an emission wavelength of ~785 nm, making it ideal for imaging in biological tissues. The sensor's high selectivity for Zn^{2+} over other structurally similar cations, such as Cd^{2+}, makes it a promising tool for monitoring zinc ion levels in biological systems. Given the high concentration of zinc in thrombi, this sensor could provide a useful tool for *in vivo* thrombus imaging.

1. Introduction

Zinc is the second most abundant transition-metal ion in the human body [1], and plays a crucial role in various biological processes as a component of enzymes and proteins [2–4]. Dysregulation of free zinc metabolism has been associated with numerous pathological states, including Alzheimer's disease, epilepsy, Parkinson's disease, ischemic stroke, thrombus, and infantile diarrhea [5–8]. The total plasma concentration of zinc ranges from 10 to 20 μM, with a significant portion bound to albumin and other proteins [9,10], leaving only a small fraction in the free, unbound state, typically 0.5–1 μM [11–14]. Platelets have the ability to actively accumulate and store zinc in their cytoplasm and α-granules [14–16], resulting in a much higher concentration of zinc in platelets compared to plasma, typically 30- to 60-fold higher [17]. Platelets themselves are known to accumulate at the site of thrombus formation [18], with concentrations in the clot up to 100-fold higher than in the circulating blood; furthermore, platelet activation can cause transient zinc release, resulting in a surge of free zinc ions in the clots [17,19–21]. Therefore, the mechanism of thrombus with the zinc surge makes zinc an ideal target for clot imaging.

Fluorescent sensors have emerged as a powerful tool for monitoring biological species *in vitro* and *in vivo* [22–25] due to their simplicity and high sensitivity [26–29]. To be ideal, a sensor should emit enhanced signals upon selective interaction with the analyte [30,31] and exhibit a large Stokes' shift to minimize self-absorption and measurement error caused by self-absorption and scattered excitation light [32,33]. For *in vivo* applications, the sensor should give optical signals in the near infrared (NIR) region (700–900 nm) to penetrate more deeply into biological tissues, with low autofluorescence interference and tissue photodamage [34–41]. As an active area of research, fluorescent probes for Zn^{2+} have made significant progress [42,43], with many turn-on and ratiometric Zn^{2+} sensors having been developed using various strategies [44–46]. Despite their attractive features, fluorescent zinc sensors have some significant drawbacks, such as intrinsic signals from autofluorescence and scattered light, which increase background noise and reduce signal fidelity [47]. Although

* Corresponding author. Gordon Center for Medical Imaging, Department of Radiology, Massachusetts General Hospital, Harvard Medical School, Boston, USA.
** Corresponding author. Department of Chemistry, The University of Akron, Akron, OH 44325, USA.
E-mail addresses: jwang83@mgh.harvard.edu (J. Wang), yp5@uakron.edu (Y. Pang).
[1] These authors contributed equally to this work.

https://doi.org/10.1016/j.jpha.2023.11.010

researchers have pursued approaches such as NIR emission, reducing background noise remains an unresolved problem due to the small spectral shift [47–49]. Hence, the challenge lies in developing a Zn^{2+} sensor that not only displays desirable NIR emission but also possesses a high selectivity and a large Stokes' shift while being unaffected by structurally similar cations, such as Cd^{2+}. In this study, we present a Zn^{2+}-selective two-photon NIR fluorescence turn-on sensor ($\lambda_{em} \approx 785$ nm) that can be excited from 900 to 1000 nm, with a large Stokes' shift (~300 nm). The sensor can detect zinc ions with high selectivity, sensitivity with high contrast.

2-(2′-Hydroxyphenyl)benzoxazole (HBO) has emerged to be an interesting component in the sensor design, due to its ability to enable the excited-state intramolecular proton transfer (ESIPT) that leads to emission with a large Stokes' shift (ca. 150–200 nm) [50–52]. Most of the reported mono-benzoxazole derivatives give blue to green emissions [53]. Our recent discovery reveals that mono-benzoxazole Schiff base **1a** could selectively bind zinc to give dual emission, resulting from its *enol* (strong green emission) and *keto* tautomers (weak NIR emission) [54]. However, the *enol* emission predominates in all solvents tested and the NIR signal is quite weak (Figs. 1A and B). In this article, we are delighted to disclose that compound **1b** binding with zinc gave strong NIR signal in nonpolar solvents (e.g., dichloromethane (DCM) and chloroform), and strong *enol* emission in polar solvents such as water or EtOH. The strong NIR emission in non-polar environment makes the probe promising to detect zinc ion *in vivo*. To verify the application of the probe, we applied the probe in cell and worm imaging. We disclose here compound **1b** is highly zinc selective cell permeable probe, giving strong NIR emission in both cell and *Caenorhabditis elegans* (*C. elegans*) imaging. As a unique feature, the probe can use both excitation and emission photons in the NIR range, which makes it an ideal zinc probe for *in vivo* imaging of biological samples, which was further proved in stroke animal models.

2. Materials and methods

2.1. Chemicals and materials

All chemicals and solvents were purchased commercially and used without further purification. All biologically evaluated compounds were isolated in ≥95% purity A.

2.2. Synthesis of compound 1b

Syntheses of the key intermediates and compound **1b** are detailed in the Supplementary data. The synthetic procedures were based on our previous methods [54].

2.3. Spectroscopic measurements

Nuclear magnetic resonance (NMR) spectra were collected on a Varian 300 Gemini spectrometer (Varian,). Mass spectrometric data were obtained on a HP1100LC/MSD mass spectrometry (Agilent, Santa Clara, CA, USA). High resolution mass spectrometry (HRMS) data were performed on an electrospray ionization time-of-flight mass spectrometry (ESI-TOF MS) system (Waters, Milford, MA, USA). Ultraviolet-visible spectroscopy (UV-Vis) spectra were acquired on a Hewlett-Packard 8453 diode-array spectrometer (Agilent, Waldbronn, Germany). Fluorescence spectra were obtained on a HORIBA Jobin Yvon NanoLog spectrometer (HORIBA Scientific, Longjumeau, France).

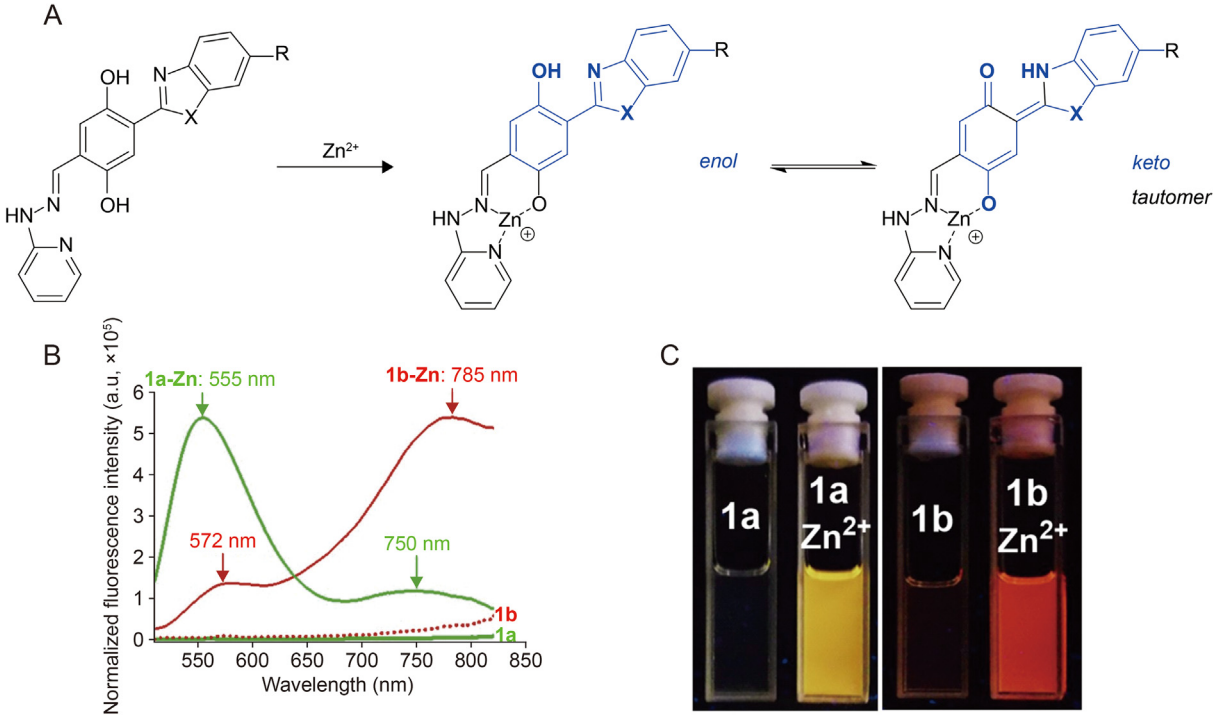

Fig. 1. (A) Structures of 2-(2′-hydroxyphenyl)benzoxazole (HBO) derivatives **1a** and **1b** and their zinc complexes. (B) Fluorescence spectra of **1a**, **1b** (10 μM) and their zinc complexes (10 μM) **1a-Zn**$^{2+}$ and **1b-Zn**$^{2+}$ in dichloromethane (DCM) (excited at 450 nm for **1a** and **1a-Zn,** and 460 nm for **1b** and **1b-Zn**). (C) The corresponding images taken under a ultraviolet (UV) lamp (365 nm) in a dark room.

3. Results and discussion

3.1. Probe design rationale

Our previous discovery has shown that the substituents (R) on the bis-benzoxazole rings could have a significant impact on *keto* emission [55,56]. And we were particularly encouraged by our recent finding that compound **1a** could selectively bind Zn^{2+}, resulting in dual emission at 555 nm (major) and 750 nm (minor) [54]. Building on this, we hypothesized that the Schiff base could be further modified to improve the NIR response. To test this, we synthesized a series of derivatives (details undisclosed), and we were pleased to find that the benzothiazole derivative **1b**-Zn produced very strong NIR emission at 785 nm, with weaker green-yellow emission at 572 nm in DCM (as shown in Figs. 1B and C). Our results reveal a significant heteroatom substitution effect that greatly enhances the NIR emission of the sensor.

3.2. Synthesis and validation of the probe 1b

The synthesis of **1b** was achieved by reacting 2-hydrozinylpyridine with the corresponding aldehyde, resulting in 97% yield (Scheme S1, ESI†). Ligand **1b** displayed an absorption band with $\lambda_{max} = 425$ nm in EtOH. The addition of Zn^{2+} resulted in a progressive decrease of the absorption band, accompanied by the appearance of a new band at approximately 477 nm (Fig. S1, ESI†). The observed bathochromic shift indicated deprotonation, resulting from Zn^{2+} binding to the phenol group. A distinct isosbestic point at around 443 nm suggested that Zn^{2+} binding produced a single new chemical species. The signal change reached completion upon the addition of one equivalent Zn^{2+}, indicating a 1:1 ligand-to-metal ratio, which was also supported by Job's plot (Fig. S2, ESI†) and ESI-TOF MS^+ data. ESI mass spectroscopy identified the mass 424.9564, corresponding to [**1b** + Zn^{2+} − H^+]$^+$, which is in agreement with the calculated mass for $C_{19}H_{13}N_4O_2SZn$: 425.0414 (Fig. 2 and Fig. S3, ESI†).

3.3. Response of probe 1b

The response of sensor **1b** to zinc ions was investigated in HEPES buffer (10 mM, pH = 7.2) containing 50% EtOH (Fig. S4, ESI†). Consistent with expectations, **1b** produced weak fluorescence at 637 nm (φ_{fl} = 0.05). However, upon addition of Zn^{2+} cations, the fluorescence was significantly enhanced (φ_{fl} = 0.57). Notably, **1b**-Zn^{2+} exhibited a solvent-switchable property, and the *enol* and *keto* emission of **1b**-Zn^{2+} in different solvents were investigated to gain insight into its properties (Fig. 3A). Specifically, **1b**-Zn^{2+} was found to be highly sensitive to solvent polarity, with non-polar solvents like DCM favoring *keto* emission, while polar solvents favored *enol* emission (Figs. 3A and S4, ESI†). In contrast, **1a**-Zn^{2+} showed no significant influence of solvent polarity on its *enol* and *keto* emission (Fig. 3B). These results indicate that the ratio of *enol* and *keto* emission from **1b**-Zn^{2+} is more responsive to its environment, which offers new opportunities for studying and understanding biological environments.

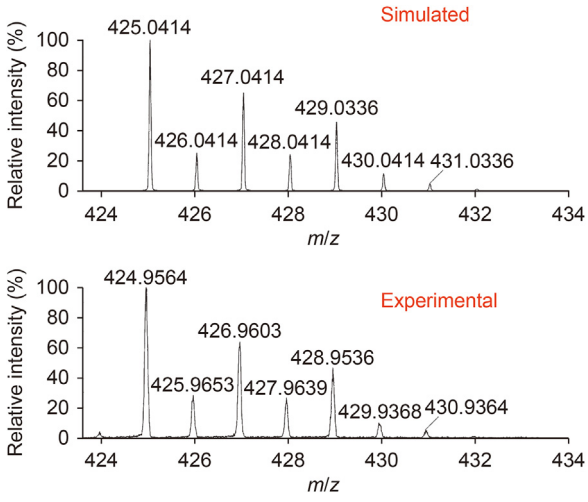

Fig. 2. Electrospray ionization time-of-flight mass spectrometry (ESI-TOF $MS)^+$ of **1b**-Zn^{2+}.

3.4. Selectivity of probe 1b

To explore the selectivity of **1b** especially its ability to differentiate cadmium sensing, we investigated the fluorescence spectra of **1b** upon addition of 5.0 equivalents of various metal ions in HEPES buffer (10 mM, pH = 7.2) containing 50% EtOH. Probe **1b** exhibited no response to physiologically important ions such as K^+, Na^+, and Ca^{2+} (Fig. 4A). To further investigate the selectivity of probe **1b**, competitive experiments were carried out using 5.0 equivalents of Zn^{2+} and one of the other metal ions (Fig. S5, ESI†). Impressively, the sensor did not display any observable fluorescence response to Cd^{2+}, which typically interferes with Zn^{2+} detection in most reported zinc sensors [4–8]. With the exception of Cu^{2+}, nearly all tested transition metals known as fluorescence quenchers did not interfere with zinc detection (Fig. 4B). Thus, **1b** exhibited excellent selectivity towards Zn^{2+}, inducing both fluorescence turn-on and a large spectral shift. In addition, **1b** demonstrated a linear response towards zinc within the range of 40–700 nM in the buffered aqueous (10 mM, pH = 7.2), with a detection limit as low as 10 nM (Fig. S6, ESI†). Taken together, these findings indicate that **1b** is a reliable and selective sensor for zinc cation. Additionally, the two photon excitable feature of **1b**-Zn (Fig. S7, ESI†) makes it promising for *in vivo* two photon fluorescent imaging.

3.5. Imaging of probe 1b in Hela cells

The remarkable selectivity of sensor **1b** to Zn^{2+} and its solvent-switchable property make it an excellent candidate for fluorescent sensing of zinc cation in cells. To test this, the probe was applied to cell imaging to detect intracellular Zn^{2+} in Hela cells (Fig. 5). Initially, weak fluorescence was observed in cells treated with only dye **1b** (Fig. 5C). However, when the cells were treated with both Zn^{2+} and dye **1b**, strong NIR fluorescence turn-on was observed from the cell imaging in the cytoplasm (Fig. 5F). This strong signal suggests that the probe can penetrate the cell membrane and form **1b**-Zn^{2+} in relatively non-polar/hydrophobic environments, which is similar to the emission of **1b**-Zn^{2+} in DCM. It is widely accepted that organic probes have a high tendency to accumulate in the hydrophobic regions of cells, which may explain the ability of the probe to penetrate the cells and bind to intracellular Zn^{2+} to emit strong NIR fluorescent light [57]. Overall, these results demonstrate that the probe is highly suitable for determining intracellular Zn^{2+} for *in vivo* imaging applications.

3.6. In vivo imaging of probe 1b in C. elegans

The *in vivo* imaging of Zn^{2+} using sensor **1b** was further validated in *C. elegans*. The experiment was conducted in two different media: a zinc-free medium and a zinc-rich medium with a concentration of 10 μM $Zn(OAC)_2$. In the zinc-free medium, only weak signals were observed in both the green and NIR windows (Figs. 6A–D). However, when the *C. elegans* were cultured in the zinc-

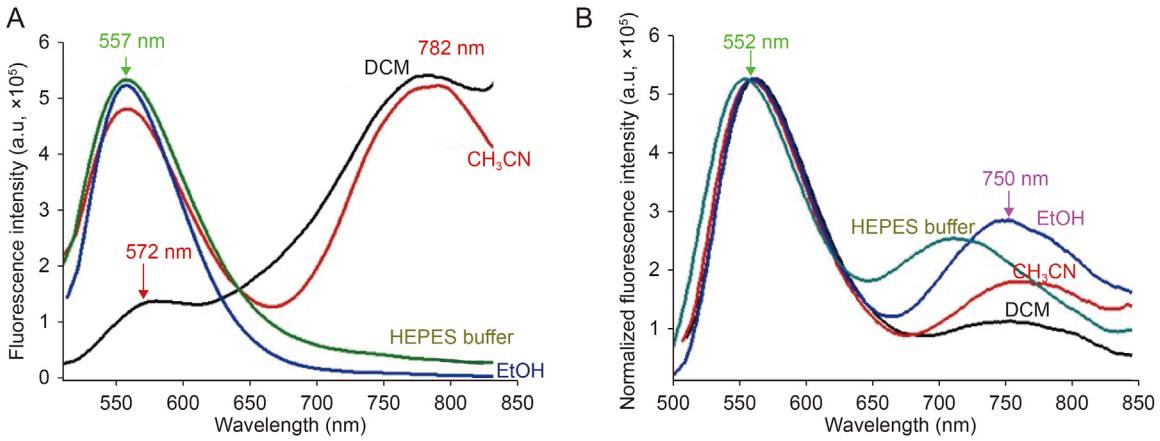

Fig. 3. Normalized fluorescence emission of (A) **1b-Zn** (10 μM) complex excited at 490 nm and (B) **1a-Zn** (10 μM) complex excited at 450 nm in different solvents. DCM: dichloromethane.

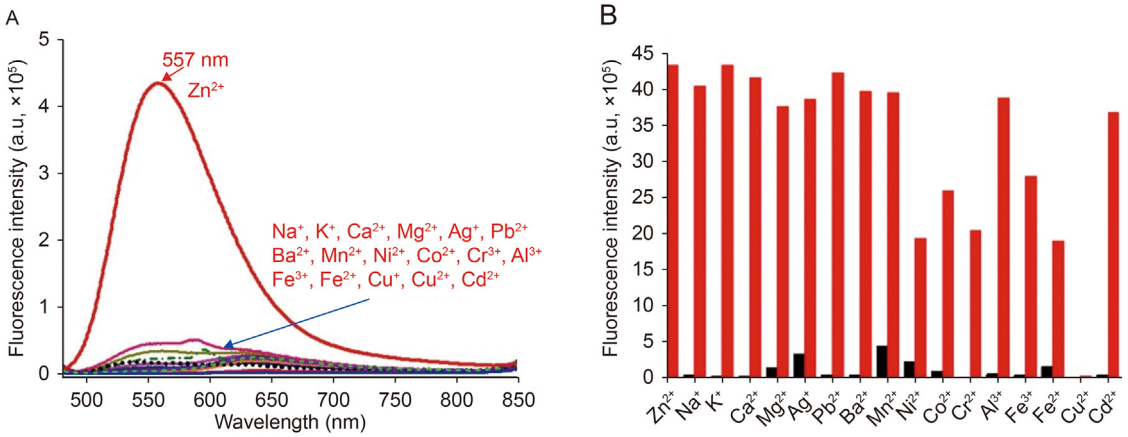

Fig. 4. (A) Fluorescence spectra of **1b** (10 μM) in HEPES buffer (10 mM, pH = 7.2) containing 50% EtOH upon addition of 5.0 equiv. of different metal ions excited at 460 nm. (B) Selective and competitive experiments of **1b** (10 μM) in EtOH:HEPES (10 mM) = 1:1 (*V/V*) (pH = 7.2). Black bars: fluorescence intensity of **1b** (10 μM) in the presence of 5.0 equiv. of corresponding metal ions only; Red bars: fluorescence intensity of **1b** (10 μM) in the presence of 5.0 equiv. of corresponding metal ions and Zn^{2+} ions.

rich medium, strong zinc signals were detected in the NIR window upon excitation at 950 nm (Figs. 6E–H). These results further confirmed the ability of sensor **1b** to detect zinc *in vivo* and its potential for use in two-photon imaging. The use of two-photon imaging allows for deep tissue imaging with high spatial resolution and reduced phototoxicity. Therefore, sensor **1b** could be a valuable tool for studying zinc homeostasis and other biological processes *in vivo*.

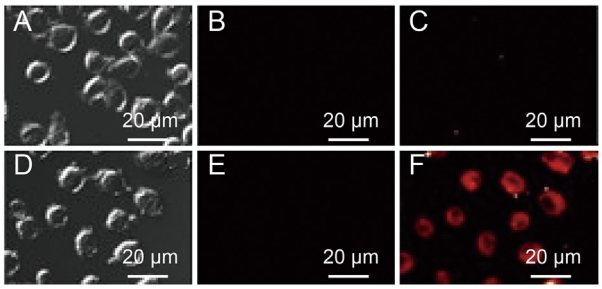

Fig. 5. Fluorescence images of Zn^{2+} detection in Hela cells were collected on an Olympus spectral confocal microscopy (Olympus Life Science, Waltham, MA, USA) excited with a 488 nm laser. (A–C): cells exposed to 10 μM dye **1b** for 30 min (control group). (D–F): cells exposed to 30 μM Zn^{2+} for 30 min, then washed with phosphate buffered saline (PBS) 3 times and further incubated with 10 μM dye **1b** in PBS for another 30 min. We employed identical confocal settings as those used for compound **1a**, which exhibited a very strong green signal in our previous publication [54]. The images were collected at bright field (A and D), green channel (B and E) and near infrared (NIR) channel (C and F, 700–800 nm).

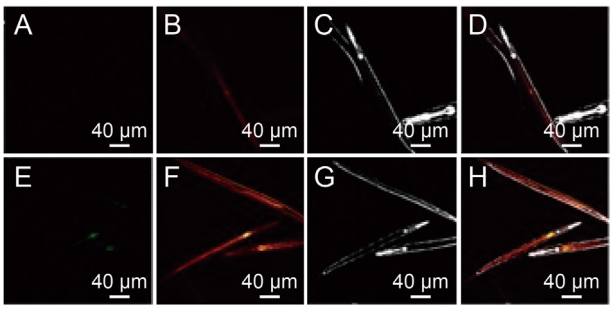

Fig. 6. Fluorescence images of Zn^{2+} detection in *C. elegans* were collected on an Olympus FV1000 multiphoton confocal microscope (Olympus Life Science, Waltham, MA, USA) excited with a 950 nm laser, and the near infrared (NIR) emission window was from 700 to 800 nm. 10 μM dye **1b** was used in this experiment. We employed identical confocal settings as those used for compound **1a** [54]. (A–D): *C. elegans* were cultured in a zinc free medium. (E–H): *C. elegans* were cultured in a zinc rich medium (10 μM).

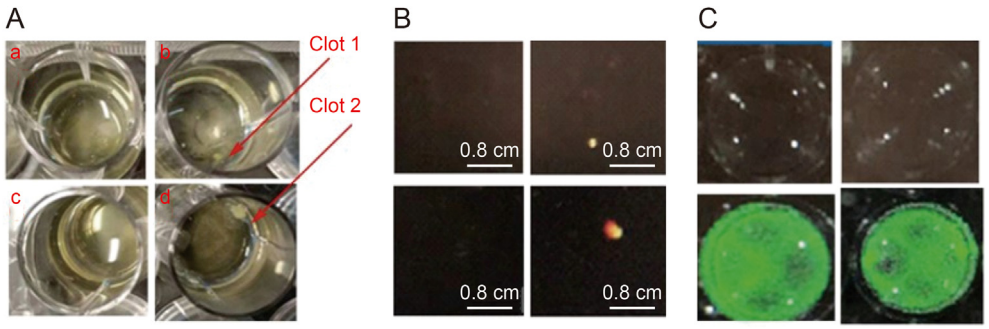

Fig. 7. *In vitro* thrombus imaging using 10 μM dye **1b** with and without Zn^{2+} (10 μM). (A) Bright filed. (B) Near infrared (NIR) channel. (C) Green channel. In Fig. 7A, (a) Human plasma + **1b**. (b) Human plasma + **1b** + thrombin. (c) Human plasma + **1b** + Zn^{2+}. (d) Human plasma + **1b** + Zn^{2+} + thrombin. The samples were imaged with Ex/Em = 465/560 nm (Green channel) or Ex/Em = 465/760 nm (NIR channel) using an IVIS® spectrum imaging system (PerkinElmer, Inc. Waltham, MA, USA).

3.7. *In vitro imaging of thrombus*

To explore the potential of the zinc probe for thrombus imaging in disease models, an *in vitro* thrombus model was initially employed for further investigation [58–60]. In a zinc-rich medium, the thrombin-induced clot was significantly larger than the one formed without the addition of zinc (Fig. 7A). The results clearly indicated the important role of zinc in thrombus formation. These findings are consistent with previous reports indicating that Zn^{2+} accelerates thrombin-mediated clotting in plasma, leading to an increase in fiber diameter and changes in overall clot structure [59]. These results highlight the significance of zinc in thrombus formation and suggest that the probe may be useful for detecting and monitoring thrombus formation *in vivo*. Additionally, the thrombus imaging results showed that the new probe produced significant fluorescence turn-on signals within the clots in the NIR channel, with high contrast (Fig. 7B). Interestingly, in the zinc-rich plasma, the free zinc in aqueous gave a bright green signal, which made it difficult to distinguish the clot in the green channel, or alternatively, we can assume that the green emission is relatively weak within the clot (Fig. 7C). This finding suggests that the clot is quite hydrophobic, and **1b**-Zn^{2+} in the clot may exhibit similar properties to those observed in DCM, that is strong NIR emission. Therefore, we can say this probe is highly enviromentally sensitive and all these results provide further evidence that the new probe has great potential for *in vivo* thrombus imaging applications.

3.8. *In vivo imaging of stroke*

Following the successful *in vitro* experiments of thrombus imaging, the probe was tested for *in vivo* stroke imaging in C57BL/6J mice (22–25 g) using a laser-induced stroke model [61,62]. The mice received an injection of probe **1b** through the tail vein (10 μM in saline with 10% dimethyl sulfoxide (DMSO); 100 μL/10 g). Subsequently, the vessels situated 50 μm beneath the skull were observed using a two-photon microscope. Zinc staining was clearly observed in some cells along the blood vessels (red signal, Fig. 8),

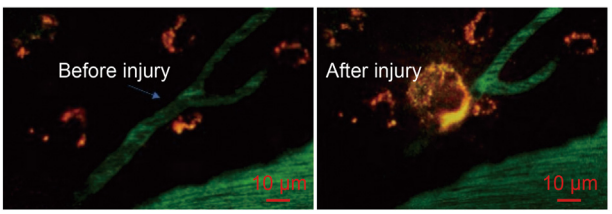

Fig. 8. *In vivo* stroke imaging in C57BL/6J mice by a two-photon microscope (excited with a 900 nm laser). After the injury, we can see the vessel was blocked.

confirming successful uptake of the probe by the cells. This was further validated by injection of fluorescein isothiocyanate (FITC) (green signal), highlighting the blood vessels. High laser power (900 nm with 100% of the power) was then locally applied to one of the vessels for 2 s to injure the blood vessel, resulting in the leakage and formation of a blood clot, which were clearly imaged with a strong red signal with high contrast. These results demonstrate the potential of this probe for *in vivo* drug screening, as it allows for real-time imaging of clot formation in the brain (See the video in the Supplementary data).

4. Conclusion

In summary, the development of a highly selective sensor for zinc cation was successfully demonstrated in this study. The sensor design utilized the Schiff base in the zinc-binding event, resulting in a large fluorescence response through the ESIPT of HBO **1b**. Unlike other sensors, this new sensor not only generates a large fluorescence NIR turn-on at ~782 nm but also with a large Stokes' shift (~300 nm). The zinc complex **1b**-Zn^{2+} exhibited sensitivity to solvent polarity with the *keto* **e**mission favored in non-polar solvent DCM and the *enol* emission favored in polar solvents. The sensor was also able to produce clear NIR imaging of Zn^{2+} in both Hela cells and *C. elegans*. Furthermore, the probe was effectively utilized in the *in vitro* and *in vivo* imaging of thrombus. The *in vitro* study showed that the addition of zinc to the thrombus model resulted in a larger clot size and significant fluorescence turn-on signals within the clots in the NIR channel. In the *in vivo* stroke model, the probe was administered *via* tail vein. After inducing the blood clots, a strong signal from the clot was also seen in the real-time imaging. These successful results suggest that the probe could potentially enable both *in vivo* thrombus imaging and drug screening for thrombus-related diseases.

Ethic statement

All animal experiment procedures were complied with the Guide for the Care and Use of Laboratory Animals and were approved by the Animal Experimentation Committee of Hainan Medical University Graduate School (Approval number: HYLL-2021-140; approval date: April 12, 2021).

CRediT author statement

Junfeng Wang: Investigation, Methodology, Data curation, Formal analysis, Writing - Original draft preparation; **Qibing Liu**: Methodology, Animal imaging, Data curation, Writing - Reviewing

and Editing; **Yingbo Li**: Investigation, Cell culture, Confocal Imaging, Data curation, Writing - Reviewing and Editing; **Yi Pang**: Supervision, Conceptualization, Project administration, Writing - Reviewing and Editing, Funding acquisition.

Declaration of competing interest

The authors declare that there are no conflicts of interest.

Acknowledgments

This work was supported by National Institute of Health (Grant Nos.: 1R15EB014546-01A1 and K25AG061282). We also thank the Coleman endowment from the University of Akron for partial support.

Appendix A. Supplementary data

Supplementary data to this article can be found online at https://doi.org/10.1016/j.jpha.2023.11.010.

References

[1] N.C. Lim, H.C. Freake, C. Brückner, Illuminating zinc in biological systems, Chemistry 11 (2004) 38–49.
[2] L.A. Finney, T.V. O'Halloran, Transition metal speciation in the cell: insights from the chemistry of metal ion receptors, Science 300 (2003) 931–936.
[3] C.E. Outten, T.V. O'Halloran, Femtomolar sensitivity of metalloregulatory proteins controlling zinc homeostasis, Science 292 (2001) 2488–2492.
[4] J.M. Berg, Y. Shi, The galvanization of biology: A growing appreciation for the roles of zinc, Science 271 (1996) 1081–1085.
[5] C. Fischer Walker, R.E. Black, Zinc and the risk for infectious disease, Annu. Rev. Nutr. 24 (2004) 255–275.
[6] J.Y. Lee, T.B. Cole, R.D. Palmiter, et al., Contribution by synaptic zinc to the gender-disparate plaque formation in human Swedish mutant APP transgenic mice, Proc. Natl. Acad. Sci. USA 99 (2002) 7705–7710.
[7] J.Y. Koh, S.W. Suh, B.J. Gwag, et al., The role of zinc in selective neuronal death after transient global cerebral ischemia, Science 272 (1996) 1013–1016.
[8] A.I. Bush, W.H. Pettingell, G. Multhaup, et al., Rapid induction of Alzheimer A beta amyloid formation by zinc, Science 265 (1994) 1464–1467.
[9] P. Zalewski, A. Truong-Tran, S. Lincoln, et al., Use of a zinc fluorophore to measure labile pools of zinc in body fluids and cell-conditioned media, Biotechniques 40 (2006) 509–520.
[10] T. Kambe, T. Tsuji, A. Hashimoto, et al., The physiological, biochemical, and molecular roles of zinc transporters in zinc homeostasis and metabolism, Physiol. Rev. 95 (2015) 749–784.
[11] J. Lu, A.J. Stewart, P.J. Sadler, et al., Albumin as a zinc carrier: Properties of its high-affinity zinc-binding site, Biochem. Soc. Trans. 36 (2008) 1317–1321.
[12] D.C. Chilvers, J.B. Dawson, M.H. Bahreyni-Toosi, et al., Identification and determination of copper- and zinc-protein complexes in blood plasma after chromatographic separation on DEAE-Sepharose CL-6B, Analyst 109 (1984) 871–876.
[13] J.W. Foote, H.T. Delves, Distribution of zinc amongst human serum proteins determined by affinity chromatography and atomic-absorption spectrophotometry, Analyst 108 (1983) 492–504.
[14] B.L. Vallee, K.H. Falchuk, The biochemical basis of zinc physiology, Physiol. Rev. 73 (1993) 79–118.
[15] S. Kiran Gotru, J.P. van Geffen, M. Nagy, et al., Defective Zn^{2+} homeostasis in mouse and human platelets with α- and δ-storage pool diseases, Sci. Rep. 9 (2019), 8333.
[16] G. Marx, G. Korner, X. Mou, et al., Packaging zinc, fibrinogen, and factor XIII in platelet alpha-granules, J. Cell. Physiol. 156 (1993) 437–442.
[17] D.B. Milne, N.V. Ralston, J.C. Wallwork, Zinc content of cellular components of blood: Methods for cell separation and analysis evaluated, Clin. Chem. 31 (1985) 65–69.
[18] D.S. Sim, G. Merrill-Skoloff, B.C. Furie, B. Furie, et al., Initial accumulation of platelets during arterial thrombus formation in vivo is inhibited by elevation of basal cAMP levels, Blood 103 (2004) 2127–2134.
[19] G. Apodaca, Modulation of membrane traffic by mechanical stimuli, Am. J. Physiol. Ren. Physiol. 282 (2002) F179–F190.
[20] P.P. Lemons, D. Chen, S.W. Whiteheart, Molecular mechanisms of platelet exocytosis: requirements for alpha-granule release, Biochem. Biophys. Res. Commun. 267 (2000) 875–880.
[21] A. du P. Heyns, A. Eldor, R. Yarom, et al., Zinc-induced platelet aggregation is mediated by the fibrinogen receptor and is not accompanied by release or by thromboxane synthesis, Blood 66 (1985) 213–219.
[22] Z. Guo, G.H. Kim, I. Shin, et al., A cyanine-based fluorescent sensor for detecting endogenous zinc ions in live cells and organisms, Biomaterials 33 (2012) 7818–7827.
[23] H.N. Kim, Z. Guo, W. Zhu, et al., Recent progress on polymer-based fluorescent and colorimetric chemosensors, Chem. Soc. Rev. 40 (2011) 79–93.
[24] X. Chen, T. Pradhan, F. Wang, et al., Fluorescent chemosensors based on spiroring-opening of xanthenes and related derivatives, Chem. Rev. 112 (2012) 1910–1956.
[25] D.W. Domaille, E.L. Que, C.J. Chang, Synthetic fluorescent sensors for studying the cell biology of metals, Nat. Chem. Biol. 4 (2008) 168–175.
[26] N. Boens, V. Leen, W. Dehaen, Fluorescent indicators based on BODIPY, Chem. Soc. Rev. 41 (2012) 1130–1172.
[27] M.S. Gonçalves, Fluorescent labeling of biomolecules with organic probes, Chem. Rev. 109 (2009) 190–212.
[28] A. Loudet, K. Burgess, BODIPY dyes and their derivatives: Syntheses and spectroscopic properties, Chem. Rev. 107 (2007) 4891–4932.
[29] J.W. Lichtman, J.-A. Conchello, Fluorescence microscopy, Nat. Methods 2 (2005) 910–919.
[30] Z. Xu, J. Yoon, D.R. Spring, Fluorescent chemosensors for Zn(2+), Chem. Soc. Rev. 39 (2010) 1996–2006.
[31] A.P. de Silva, H.Q. Gunaratne, T. Gunnlaugsson, et al., Signaling recognition events with fluorescent sensors and switches, Chem. Rev. 97 (1997) 1515–1566.
[32] X. Peng, F. Song, E. Lu, et al., Heptamethine cyanine dyes with a large stokes shift and strong fluorescence: A paradigm for excited-state intramolecular charge transfer, J. Am. Chem. Soc. 127 (2005) 4170–4171.
[33] Z. Zhang, S. Achilefu, Synthesis and evaluation of polyhydroxylated near-infrared carbocyanine molecular probes, Org. Lett. 6 (2004) 2067–2070.
[34] H. Kobayashi, M. Ogawa, R. Alford, et al., New strategies for fluorescent probe design in medical diagnostic imaging, Chem. Rev. 110 (2010) 2620–2640.
[35] D.J. Hawrysz, E.M. Sevick-Muraca, Developments toward diagnostic breast cancer imaging using near-infrared optical measurements and fluorescent contrast agents, Neoplasia 2 (2000) 388–417.
[36] L. Yuan, W. Lin, S. Zhao, et al., A unique approach to development of near-infrared fluorescent sensors for in vivo imaging, J. Am. Chem. Soc. 134 (2012) 13510–13523.
[37] N. Karton-Lifshin, E. Segal, L. Omer, et al., A unique paradigm for a Turn-ON near-infrared cyanine-based probe: Noninvasive intravital optical imaging of hydrogen peroxide, J. Am. Chem. Soc. 133 (2011) 10960–10965.
[38] D. Oushiki, H. Kojima, T. Terai, et al., Development and application of a near-infrared fluorescence probe for oxidative stress based on differential reactivity of linked cyanine dyes, J. Am. Chem. Soc. 132 (2010) 2795–2801.
[39] S.A. Hilderbrand, R. Weissleder, Near-infrared fluorescence: Application to in vivo molecular imaging, Curr. Opin. Chem. Biol. 14 (2010) 71–79.
[40] J. Frangioni, In vivo near-infrared fluorescence imaging, Curr. Opin. Chem. Biol. 7 (2003) 626–634.
[41] R. Weissleder, A clearer vision for in vivo imaging, Nat. Biotechnol. 19 (2001) 316–317.
[42] K. Kikuchi, K. Komatsu, T. Nagano, Zinc sensing for cellular application, Curr. Opin. Chem. Biol. 8 (2004) 182–191.
[43] E.M. Nolan, S.J. Lippard, Small-molecule fluorescent sensors for investigating zinc metalloneurochemistry, Acc. Chem. Res. 42 (2009) 193–203.
[44] P. Jiang, Z. Guo, Fluorescent detection of zinc in biological systems: Recent development on the design of chemosensors and biosensors, Coord. Chem. Rev. 248 (2004) 205–229.
[45] T. Wu, M. Kumar, J. Zhang, et al., A genetically encoded far-red fluorescent indicator for imaging synaptically released Zn^{2+}, Sci. Adv. 9 (2023), eadd2058.
[46] K.H. Alharbi, A review on organic colorimetric and fluorescent chemosensors for the detection of Zn(II) Ions, Crit. Rev. Anal. Chem. 53 (2023) 1472–1488.
[47] Y. You, S. Lee, T. Kim, et al., Phosphorescent sensor for biological mobile zinc, J. Am. Chem. Soc. 133 (2011) 18328–18342.
[48] X. Zhang, K.S. Lovejoy, A. Jasanoff, et al., Water-soluble porphyrins as a dual-function molecular imaging platform for MRI and fluorescence zinc sensing, Proc. Natl. Acad. Sci. USA 104 (2007) 10780–10785.
[49] K. Kiyose, H. Kojima, Y. Urano, et al., Development of a ratiometric fluorescent zinc ion probe in near-infrared region, based on tricarbocyanine chromophore, J. Am. Chem. Soc. 128 (2006) 6548–6549.
[50] S. Hillebrand, M. Segala, T. Buckup, et al., First hyperpolarizability in proton-transfer benzoxazoles: Computer-aided design, synthesis and study of a new model compound, Chem. Phys. 273 (2001) 1–10.
[51] P. Chou, M.L. Martinez, J.H. Clements, Reversal of excitation behavior of proton-transfer vs. charge-transfer by dielectric perturbation of electronic manifolds, J. Phys. Chem. 97 (1993) 2618–2622.
[52] A.S. Klymchenko, A.P. Demchenko, Electrochromic modulation of excited-state intramolecular proton transfer: The new principle in design of fluorescence sensors, J. Am. Chem. Soc. 124 (2002) 12372–12379.

[53] J. Seo, S. Kim, S. Park, et al., Tailoring the excited-state intramolecular proton transfer (ESIPT) fluorescence of 2-(2'-hydroxyphenyl)benzoxazole derivatives, Bull. Korean Chem. Soc. 26 (2005) 1706–1710.
[54] J. Wang, Y. Li, E. Duah, et al., A selective NIR-emitting zinc sensor by using Schiff base binding to turn-on excited-state intramolecular proton transfer, J. Mater. Chem. B 2 (2014) 2008–2012.
[55] Y. Xu, Y. Pang, Zinc binding-induced near-IR emission from excited-state intramolecular proton transfer of a bis(benzoxazole) derivative, Chem. Commun. 46 (2010) 4070–4072.
[56] Y. Xu, Q. Liu, B. Dou, et al., Zn(2+) binding-enabled excited state intramolecular proton transfer: A step toward new near-infrared fluorescent probes for imaging applications, Adv. Healthc. Mater. 1 (2012) 485–492.
[57] S. Mizukami, S. Watanabe, Y. Akimoto, et al., No-wash protein labeling with designed fluorogenic probes and application to real-time pulse-chase analysis, J. Am. Chem. Soc. 134 (2012) 1623–1629.
[58] J. Wang, H. Baumann, X. Bi, et al., Efficient synthesis of NIR emitting bis[2-(2'-hydroxylphenyl)benzoxazole] derivative and its potential for imaging applications, Bioorg. Chem. 96 (2020), 103585.
[59] S.J. Henderson, J. Xia, H. Wu, et al., Zinc promotes clot stability by accelerating clot formation and modifying fibrin structure, Thromb. Haemost. 115 (2016) 533–542.
[60] T.T. Vu, J.C. Fredenburgh, J.I. Weitz, Zinc: An important cofactor in haemostasis and thrombosis, Thromb. Haemost. 109 (2013) 421–430.
[61] M. Boyko, R. Kuts, B.F. Gruenbaum, et al., An alternative model of laser-induced stroke in the motor cortex of rats, Biol. Proced. Online 21 (2019), 9.
[62] Y. Li, J. Zhang, Animal models of stroke, Animal Model. Exp. Med. 4 (2021) 204–219.